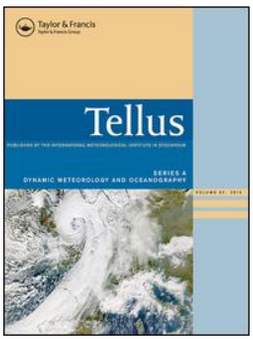

Tellus A: Dynamic Meteorology and Oceanography

ISSN: (Print) 1600-0870 (Online) Journal homepage: https://www.tandfonline.com/loi/zela20

The coupled ocean–atmosphere hydrologic cycle

Dipanjan Dey & Kristofer Döös

To cite this article: Dipanjan Dey & Kristofer Döös (2019) The coupled ocean–atmosphere hydrologic cycle, Tellus A: Dynamic Meteorology and Oceanography, 71:1, 1650413, DOI: 10.1080/16000870.2019.1650413

To link to this article: https://doi.org/10.1080/16000870.2019.1650413

Published online: 10 Aug 2019.

Tellus SERIES A DYANAMIC METEOROLOGY AND OCEANOGRAPHY
PUBLISHED BY THE INTERNATIONAL METEOROLOGICAL INSTITUTE IN STOCKHOLM

The coupled ocean–atmosphere hydrologic cycle

By DIPANJAN DEY*, and KRISTOFER DÖÖS, *Department of Meteorology, Stockholm University, Stockholm, Sweden*

(Manuscript received 23 March 2019; in final form 22 July 2019)

ABSTRACT

The freshwater cycle has in the present study been traced as one integrated process in the coupled ocean–atmosphere system for both present and possible future climates simulated with an Earth-System Model. A method based on water-mass conservation was used in order to calculate mass fluxes of water from regions of evaporation to regions of precipitation. These fluxes include not only advection of moisture by the winds but also the vertical water-mass transport due to precipitation forming hence a mass-conserved 3D water-mass transport field. Six atmospheric hydrological cells were revealed, which cross the sea surface, where they join the oceanic overturning circulation. These atmospheric water cells can be interpreted as an extension of the oceanic overturning circulation, since the otherwise open ocean streamlines at the surface continue into the atmosphere due to evaporation and back into the ocean due to precipitation. Although these atmospheric water cells are related to the usual air cells, they are only half part of the coupled water cells and located differently. The future-climate scenario shows that the mid- and high-latitude atmospheric water-mass cells will transport more moisture towards the poles as well as increase of the northward cross-Equatorial atmospheric water-mass transport.

Keywords: meridional overturning water circulation, coupled ocean–atmosphere hydrological cells, atmospheric 3D water mass fluxes including precipitation

1. Introduction

As water is a major component of the global coupled system and its availability will be a major concern for society in the future, tracing it in both the atmosphere and ocean is of great importance. The oceanic and atmospheric branches of the hydrological cycle are connected at the sea surface by evaporation, precipitation and run-off. The hydrological cycle is further affected by currents in the ocean and winds in the atmosphere, which advect and redistribute the freshwater.

According to the Clausius–Clapeyron (C–C) relation, the air can approximately hold 7% more moisture for every 1 °C rise in temperature. In a warmer climate, this would lead to an increase of global-mean evaporation and precipitation (i.e. the strength of the global water cycle) but at a lesser rate than the C–C rate due to the energy constraints (Held and Soden, 2006; Huntington, 2006). However, the moisture content and moisture transport in a warmer atmosphere will increase at a rate approximately same as the C–C rate (Lorenz and DeWeaver, 2007). The increase of atmospheric water in a warmer climate will not only affect the Earth's surface through increased evaporation and precipitation but also strengthen the entire ocean–atmosphere hydrological cycle.

One method to detect the moisture transport in the atmosphere is to vertically integrate the horizontal water-vapour mass transport (Zhu and Newell, 1998). If integrated over longer timescales, the divergence of the integrated vapour transport is equal to the average surface freshwater flux (evaporation–precipitation) (Trenberth and Guillemot, 1998; Trenberth et al., 2011). The limitation is, however, that this does not give any information of its vertical dependency, nor does it give any information of how regions are connected. The methodology used in the present study is an extension of the previous algorithm.

Another common framework for analysing the average atmospheric and oceanic circulation are mass-transport overturning stream functions (Gill and Bryan, 1971; Manabe et al., 1990; England, 1992). Figure 1 shows this Meridional Overturning Circulation (MOC) in latitude-pressure/depth coordinates. The atmospheric MOC consists of three cells through which air circulates throughout the depth of the troposphere (Manabe et al., 1975; Wetherald and Manabe, 1972). The Hadley Cells extend from the Equator to the latitude of 30° in both

Corresponding author. e-mail: dipanjan.dey@misu.su.se

Citation: Tellus A: 2019, **71**, 1650413, https://doi.org/10.1080/16000870.2019.1650413

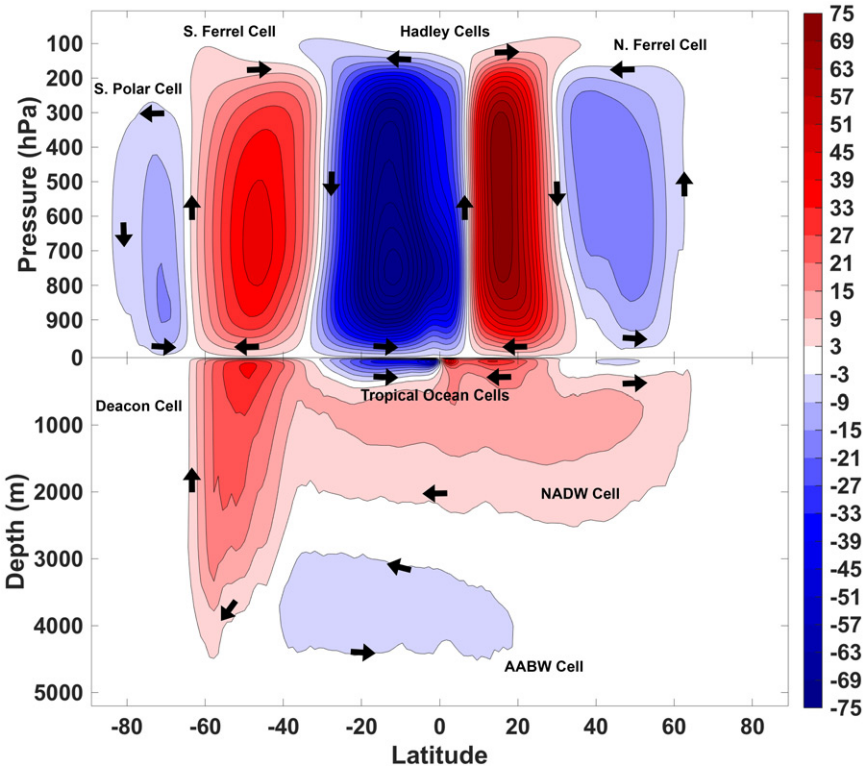

Fig. 1. The global air-mass overturning stream function for the atmosphere (top panel) and global water-mass overturning stream function for the ocean (bottom panel). Arrows indicate the mass transport direction. N represents the Northern Hemisphere and S is used for the Southern Hemisphere. NADW stands for North Atlantic Deep Water and AABW represents Antarctic Bottom Water. All transports are in Sv (10^9 kg/s).

hemispheres. These cells are located above the tropical near-surface ocean cells. The Ferrel Cells extend from 30° to 65° in both hemispheres and move in the opposite direction of that of the Hadley Cells. The southern hemispheric Ferrel Cell is found above the oceanic Deacon Cell. Further cells, known as the Polar Cells, extend from 65° to the poles. The atmospheric overturning stream functions can to some extent be used to study the hydrological cycle but it is only the oceanic one that deals directly with water. It is for this reason, we will use the atmospheric water-mass stream function of Peixoto and Oort (1992), which will not only give the net horizontal water-mass transport but also its vertical dependency with streamlines connecting the different latitudes.

The oceanic MOC consists of two near-surface tropical cells moving in opposite directions. Additionally, an intermediate cell referred to as the North Interhemispheric Cell is found between 40°S and 80°N. In the Southern Ocean, there is the Deacon Cell (Bryan, 1991), which is not a true overturning cell (Döös and Webb, 1994). A deep-ocean cell is also present, related to the presence of Antarctic Bottom Water (AABW).

The calculation of ocean overturning stream functions is obtained by integrating the meridional velocity first zonally and then vertically from the bottom of the ocean and up to the surface. This results in streamlines crossing the sea surface, which is due to the net evaporation or precipitation at different latitudes. These open streamlines are often not noticeable unless the upper metres of the ocean are visible and enough number of streamlines are graphed, since the freshwater flux across the surface does not exceed 1 Sv. These open ocean streamlines will, in the present study, be followed across the sea surface into the atmosphere by computing a water-mass stream function for the atmosphere and in this way make it possible to study the hydrological cycle as a closed loop in the coupled ocean–atmosphere system.

By using this methodology, it will be possible to detect the atmospheric water source (evaporation) and sink (precipitation) regions and how they are interconnected through the entire atmosphere and the ocean. This makes it possible to calculate the freshwater streamlines in both the ocean and the atmosphere as one integrated system expressed in the same units of kg/s of water. Thus, any change of the freshwater flux at the surface will result in an equal change of the strength of coupled ocean–atmosphere water cells.

The hydrological cycle is often described as an atmosphere-only phenomenon but is in fact only a half cycle.

The aim of the present study is to describe the complete hydrological cycle including the ocean part in the meridional–vertical plane. Although the atmospheric part of this complete hydrological cycle is one order of magnitude lower than that of the ocean, it plays a crucial role in the redistribution of salinity, which in turn determines the thermohaline circulation together with temperature.

The present study cannot predict if it is the atmosphere, the ocean or the coupled system that sets the hydrological cycle. Ferreira and Marshall (2015), however, argued that the atmospheric freshwater transport is to a large extent independent of the oceanic state. At the same time they also pointed out that to achieve the return freshwater pathway, the ocean circulation and salinity distribution must be adjusted to the atmospheric freshwater transport. Here, we will show how these two systems are connected and how the freshwater transport once beneath the sea surface merges with the oceanic overturning circulation.

The Earth System model we have used will be presented in Section 2.1. The water-mass stream function in the atmosphere will be presented in Section 2.2. In Section 3, we will discuss the obtained results of the atmospheric water-mass stream function and how it is directly connected to that of the ocean. The concluding remarks will be conferred in the final section.

2. Methods

2.1. The EC-Earth model

The simulation analysed in the present study was performed with the Earth system model EC-Earth (Hazeleger et al., 2010, 2012). The atmospheric component is based on the Integrated Forecasting System (IFS) of the European Centre for Medium Range Weather Forecasts (ECMWF). IFS is a spectral model with triangular truncation, where the T159 truncation has been used in EC-Earth, which is approximately equivalent to a 125 km (or ~1.125°) resolution. In the vertical, 62 levels of a terrain-following hybrid coordinate have been used. The lowest model level is at a height of 30 m above the ground, and the highest level is at 5 hPa.

The ocean component of EC-Earth is the NEMO model (Madec, 2008), where the ORCA1 configuration has been used, which consists of a tri-polar grid with poles over northern North America, Siberia and Antarctica at a resolution of about 1°. In order to conserve mass, the analysis was performed on this original tri-polar grid rather than on a Longitude–Latitude interpolated grid. However, the ORCA1 model grid is unstructured north of 30°N, which makes it impossible to have an exact latitude for analysis. There are 42 vertical levels defined together with a partial step representation of the bottom topography.

The analysis of the last 10 years of the historical simulation (1996–2005) was treated as the present-day climate. For the future-climate scenario, last 10 years (2091–2100) of the RCP 8.5 scenario were taken. RCP8.5 is the pathway with the highest greenhouse gas emissions among the Representative Concentration Pathways (RCPs).

2.2. The ocean–atmosphere water-mass overturning stream function

The divergence-free water-mass stream function, which will be derived here is based on water-mass conservation and has to some extent is similar to a water vapour transport function Yang et al. (2015) computed. Figure 2 provides a schematic view of how water is conserved and transported in the coupled ocean–atmosphere Earth-System Model. The water-mass in a model grid box is its air mass multiplied by its specific humidity, which yields

$$M^n_{i,j,k} = q^n_{i,j,k}\rho^n_{i,j,k}\Delta x_{i,j}\Delta y_{i,j}\Delta z^n_{i,j,k}, \tag{1}$$

where the superscript n represents the time level of the stored model fields; time is $t = n\Delta t_G$ and Δt_G is the time interval between two stored model fields. The longitudinal ($\Delta x_{i,j}$) and the latitudinal ($\Delta y_{i,j}$) grid lengths are functions of their horizontal positions i, j. The vertical coordinate in a model has a level thickness $\Delta z^n_{i,j,k}$, where the subscript k denotes the vertical level. Specific humidity ($q_{i,j,k}$) and density ($\rho_{i,j,k}$) are functions of both the horizontal positions i, j and the vertical level k. The advective horizontal water-mass transports through the eastern (U) and northern (V) faces of the i,j,k grid box at time step n are

$$U^n_{i,j,k} = q^n_{i,j,k}\rho^n_{i,j,k}u^n_{i,j,k}\Delta y_{i,j}\Delta z^n_{i,j,k}, \tag{2}$$

$$V^n_{i,j,k} = q^n_{i,j,k}\rho^n_{i,j,k}v^n_{i,j,k}\Delta x_{i,j}\Delta z^n_{i,j,k}. \tag{3}$$

The discretised hydrostatic equation yields

$$\Delta p^n_{i,j,k} = \rho^n_{i,j,k}\ g\Delta z^n_{i,j,k}, \tag{4}$$

where g is gravity and Δp is air pressure level thickness. Δp is defined to be positive, as the difference was taken in the opposite direction of Δz. The advective water-mass transports through the lateral grid faces given by equations (2), (3) will make use of equation (4) to determine Δz and hence become

$$U^n_{i,j,k} = q^n_{i,j,k}u^n_{i,j,k}\Delta y_{ij}\Delta p^n_{i,j,k}/g, \tag{5}$$

$$V^n_{i,j,k} = q^n_{i,j,k}v^n_{i,j,k}\Delta x_{i,j}\Delta p^n_{i,j,k}/g. \tag{6}$$

Conservation of water-mass yields that the rate of change of the water-mass content of a box balances the water-mass fluxes though its faces:

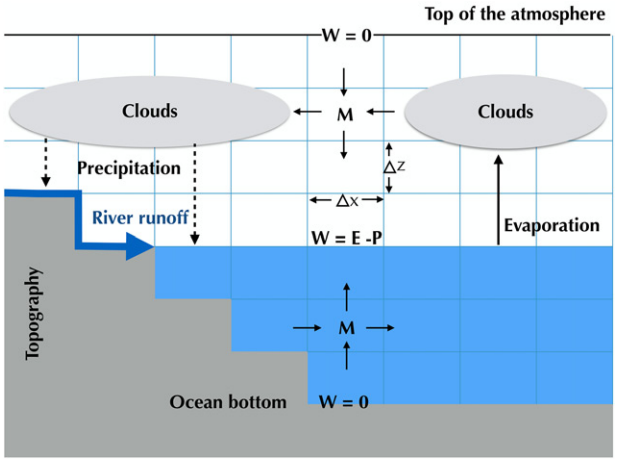

Fig. 2. Sketch of the processes that mainly regulates the coupled ocean–atmosphere hydrological cycle. Also, this schematic diagram carries detailed information about the methodology that is described in methods. M is the atmospheric water-mass in a model grid box. W is vertical water-mass transport through the upper face of the grid box and at the surface this should equal the surface freshwater flux ($E-P-R$). Conservation of water-mass yields that the rate of change of water-mass content of a box balances the water-mass fluxes though its faces.

$$\frac{\partial M_{i,j,k}}{\partial t} + U_{i,j,k} - U_{i-1,j,k} + V_{i,j,k} - V_{i,j-1,k} + W_{i,j,k} - W_{i,j,k-1} = 0, \tag{7}$$

where $W_{i,j,k}$ is the vertical water-mass transport through the upper face of the grid box. Note that this is not the equation that is integrated in the atmospheric model. Furthermore, the diffusive fluxes of moisture were neglected. Nevertheless, this water-mass conservation holds well for an analysis, which is not to be confused with a model integration, where the small errors can add up and grow. Equation (7) can be rewritten by discretising the time derivative and using the hydrostatic approximation (equation (4)):

$$\frac{\left(\Delta p^n_{i,j,k} q^n_{i,j,k} - \Delta p^{n-1}_{i,j,k} q^{n-1}_{i,j,k}\right)}{g\Delta t_G} \Delta x_{i,j} \Delta y_{i,j} + U^n_{i,j,k} - U^n_{i-1,j,k} + V^n_{i,j,k} - V^n_{i,j-1,k} + W^n_{i,j,k} - W^n_{i,j,k-1} = 0. \tag{8}$$

Values of W at all vertical levels can be computed by integrating equation (8) downwards from the top of the atmosphere (TOA), where the vertical water-mass transport is close to zero. The vertical water-mass flux is hence always computed at the bottom of each grid box successively downwards:

$$W^n_{i,j,k-1} = W^n_{i,j,k} + \left[U^n_{i,j,k} - U^n_{i-1,j,k} + V^n_{i,j,k} - V^n_{i,j-1,k} + \frac{\left(\Delta p^n_{i,j,k} q^n_{i,j,k} - \Delta p^{n-1}_{i,j,k} q^{n-1}_{i,j,k}\right)}{g\Delta t_G} \Delta x_{i,j} \Delta y_{i,j} \right]. \tag{9}$$

At the surface $W^n_{i,j,0}$ should be equal to the evaporation–precipitation (E–P). As specific humidity field only deals with the gaseous form of water and does not take into account liquid water and ice in the atmosphere, any condensation is immediately transported to the surface as precipitation. Note here that the atmospheric component of EC-Earth computes evaporation and precipitation involving many processes, but should in the end conserve the water-mass, which is what used in our method.

The meridional water-mass overturning stream function for the atmosphere can be computed if averaged over several years so that $\partial M_{i,j,k}/\partial t$ is close to zero and can be expressed in the meridional–vertical coordinates as

$$\psi^{atm}_{j,k} = \frac{1}{N} \sum_{n=1}^{N} \sum_{k'=k}^{KL} \sum_{i=1}^{IX} V^n_{i,j,k'}. \tag{10}$$

Here, N is the total number of atmospheric data 'snapshots' (10 years with 6-hourly outputs). The sea surface is represented by $k=0$ and $KL=62$ stands for the TOA. The western and eastern boundaries are given by $i=1$ and $i=IX$, respectively. The meridional air-mass stream function is calculated using the same method as described above but without the contribution from specific humidity in equation (6).

The meridional stream function for the ocean in latitude-depth coordinates (conventional ocean MOC) is calculated in the same way as in previous studies (Bryan, 1991; Döös and Webb, 1994) and can be expressed as

$$\psi^{oce}_{j,k} = -\frac{1}{N} \sum_{n=1}^{N} \sum_{k'=k}^{KM} \sum_{i=1}^{IX} VO^n_{i,j,k'}. \tag{11}$$

Here, VO is the oceanic mass transport through a meridional grid-box wall:

$$VO^n_{i,j,k'} = \rho_{oce} \; vo^n_{i,j,k'} \; \Delta x_{i,j} \Delta z^n_{i,j,k'}, \tag{12}$$

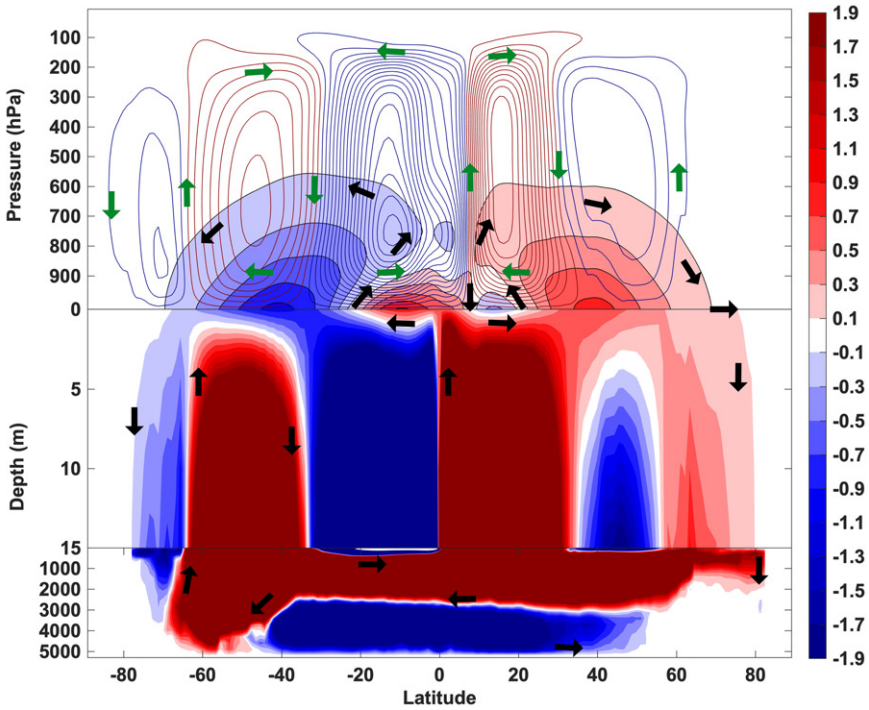

Fig. 3. The global water-mass overturning stream function for the coupled ocean–atmosphere system superimposed with the global air-mass overturning stream function for the present day climate. Black arrows show the water-mass transport direction and green arrows indicate the air-mass transport direction. All transports are in Sv (10^9 kg/s). Note that the colour scale is saturated. Contour interval for air-mass transport is 6 Sv. The ocean water-mass overturning stream function here is the same as in Fig. 1 bottom panel, but with different contour interval and with a non-linear depth scale. There are two ocean model vertical levels in the stretched part of the graph from the surface to depth 15 m.

where ρ_{oce} is the seawater density. NEMO uses the incompressibility hypothesis, which states that the three dimensional divergence of the velocity vector is assumed to be zero. This makes it possible to compute the oceanic stream function using constant sea water density. In our calculations $\rho_{oce} = 1035$ kg/m^3 and vo is the Eulerian plus eddy-induced meridional velocity from the NEMO model. The sea surface is represented by $k = 0$ and $KM = 42$ stands for the ocean bottom. N is the total number of ocean data snapshots (10 years with monthly outputs). No water-mass transport takes place through the ocean bottom and hence $\psi^{oce}_{j,KM} = 0$. The water-mass transport across the sea surface $\psi^{oce}_{j,0}$ should equal that of the atmosphere:

$$\psi^{oce}_{j,0} = \psi^{atm}_{j,0}, \tag{13}$$

which would match the $E-P-R$. The rivers will, however, transport water from the precipitation regions on land and discharge it in the ocean as a river run-off, which can result in a small discontinuity between the atmospheric and the oceanic stream lines.

The MOC can be represented using different geographical and tracer coordinate systems for both the atmosphere and ocean (Blanke et al., 2006; Ferrari and Ferreira, 2011; Döös and Nilsson, 2011; Döös et al., 2012; Zika et al., 2012). Stream function on moist isentropic coordinates was also defined to identify the role of latent heating on the atmospheric circulation (Pauluis et al., 2008, 2010). The drawback of these stream functions is, however, that the sea surface through which the atmosphere and ocean actually interact is not unique. Hence, latitude-depth coordinate system was used for the ocean and latitude-pressure framework for the atmosphere in the present study.

3. Results and discussions

3.1. Ocean–atmosphere water cells

The atmospheric water-mass overturning stream function (Fig. 3) gives us new insights regarding the atmospheric water-transport pathways and how these are connected with the oceanic overturning circulation. Figure 3 reveals six atmospheric water cells (N.B. not air cells), which connect with the oceanic overturning cells through the sea surface in terms of the large-scale freshwater circulation. Note that from the atmospheric point of view in

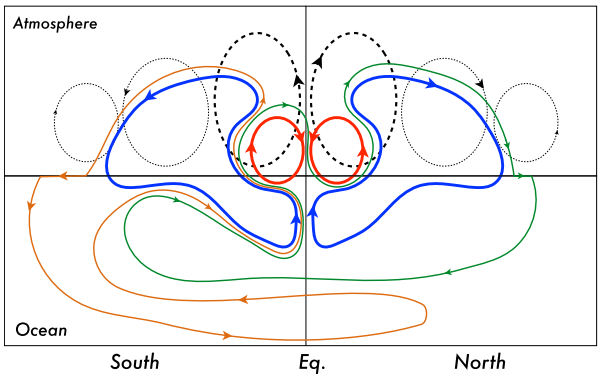

Fig. 4. Schematic diagram of the ocean–atmosphere water cells. The two Tropic Cells are in red, the two Hemispheric Cells are in blue, the North Interhemispheric Cell in green and the South Interhemispheric Cell in orange. The atmospheric air cells are superimposed in black. Note that these cells are mass budget cells and do not necessarily represent pathways of individual water parcels.

isolation there are only four cells. It is important to understand that the present analysis is a water-mass budget study. As in the case with any overturning stream function, the stream lines do not necessarily coincide with individual water particle trajectories. The first noticeable result is that the atmospheric water transport was trapped within the planetary boundary layer below 500 hPa. This is due to the fact that 90% of the atmospheric moisture is concentrated below this level (Peixoto and Oort, 1992).

The six coupled ocean–atmosphere water cells have been dubbed as the *Tropic Cells*, the *Hemispheric Cells*, the *North Interhemispheric Cell* and the *South Interhemispheric Cell* (Fig. 4). Names were given according to their spatial extent and connectivity with the overturning cells. The two Tropic Cells are extensions of the ocean-only Tropical Cells. The two Hemispheric Cells are almost spread horizontally over their respective entire hemispheres. The North Interhemispheric Cell merges with the North Atlantic Deep Water (NADW) and the South Interhemispheric Cell merges with the AABW Cell and is to a large extent located in the Southern Hemisphere (SH). Note that both the South Tropic Cell and the South Hemispheric Cell are larger in magnitude than their northern counterparts, probably since there are less land surfaces in the SH at the equivalent latitudes. Also, the atmospheric extension of the cells are symmetric just north of the Equator, which is due to the mean position of the Inter Tropical Convergence Zone (ITCZ).

The two *Tropic Cells*, illustrated by the red lines in Fig. 4, clearly show that the water-mass transports towards the ITCZ are in opposite directions to those of the air transport (thick black dashed lines). Rising air loses its moisture due to condensation and precipitation. After precipitation, the water flows poleward in the shallow ocean Ekman layer driven by the trade winds until it re-evaporates. The evaporated moisture then returns towards the ITCZ by advection of air in the lower branches of the Hadley Cells, whereafter it returns to the ocean by precipitation and closes the cells.

The two *Hemispheric Cells* are shown by the blue lines in Fig. 4. At the Equator the water upwells and then flows poleward in the shallow Ekman layers driven by the trade winds until it reaches the surface and evaporates. After evaporation, the moisture is advected equatorwards in the lower branch of the Hadley Cell (note that the streamlines are tilted towards the Equator in Fig. 3). The moisture is further advected polewards by the mid-latitude transient eddies at higher altitudes and feeds the low-pressure areas associated with the polar fronts. Note that the water streamlines do not follow the air streamlines of the Hadley and Ferrel Cells. After precipitating, the water returns equatorwards in the oceanic Ekman layer driven by the westerlies and eventually merges with the Ocean Tropical Cells. The water is then subducted and flows equatorwards along the isopycnals (constant-density surfaces) until it reaches the Equator and upwells across the isopycnals.

The *North Interhemispheric Cell* is illustrated by the green line in Fig. 4. Starting at the ITCZ, the water precipitates and flows northwards in the shallow Ekman layer until it evaporates at the sea surface. Moisture from evaporation is first advected towards the ITCZ by the lower branch of the Northern Hemisphere Hadley Cell. Near the ITCZ the moisture is transported towards higher altitudes by the Hadley Cell. Instead of precipitating at the ITCZ the moisture is further advected polewards by transient eddies. Finally, the moisture precipitates in the North Atlantic and North Pacific. After precipitation, the ocean surface water flows polewards due to the polar easterlies. It is important to note that the atmospheric moisture transport from the subtropics to higher latitudes is more noticeable in the North Pacific than in the North Atlantic through the signature of low sea surface salinity (Warren, 1983; Emile-Geay et al., 2003). In the North Atlantic Ocean, the water convects into NADW, which then flows southwards and to a large extent upwells in the Southern Ocean. The water then flows northwards in the Ekman layer until it subducts and continues equatorwards along the isopycnals until it upwells at the Equator. The upwelled ocean water at the Equator first returns southwards in the shallow oceanic Ekman layer due to the easterlies until it re-evaporates. The evaporated water is advected across the Equator and feeds the ITCZ with precipitation, which closes the North Interhemispheric Cell.

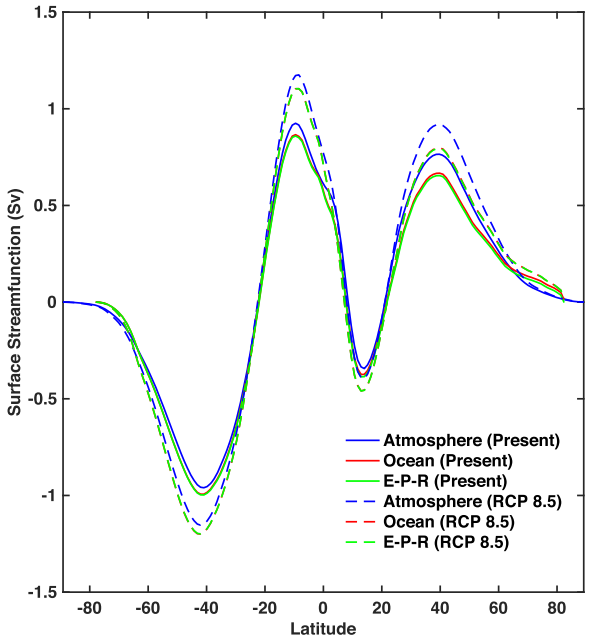

Fig. 5. Water-mass stream function at the sea surface for the atmosphere (solid blue line), the ocean (solid red line) and surface freshwater flux (solid green line) for the present day climate. The dashed lines represent the future climate (RCP 8.5 scenario).

The *South Interhemispheric Cell*, represented by the orange 'loop' in Fig. 4, is similar to the North Interhemispheric Cell but does not cross the Equator in the atmosphere. The ocean water that upwells at the Equator flows southwards in the shallow oceanic Ekman layer until it evaporates at the sea surface. After evaporation, the transport of moisture is governed by the same mechanism as in the case of the North Interhemispheric Cell until the moisture precipitates in the Southern Ocean. The precipitated water subsequently convects to great depths and merges with the AABW and then flows northwards and crosses the Equator in the abyssal ocean. Hereafter, the water rises and flows southwards until it upwells in the Southern Ocean. It then moves northwards in the oceanic Ekman layer until it subducts and continues equatorwards along the isopycnals until it upwells at the Equator, which closes the South Interhemispheric Cell.

One way to validate this atmospheric water-mass stream function is to compare it with the ocean stream function at the surface. The atmospheric water stream function is obtained by integrating downward from the top of the atmosphere to the surface. The ocean stream function is integrated in the reverse direction from the bottom of the ocean and upward to the sea surface. The only reason they would not be identical at the surface is that the precipitated water on land is transported by the rivers out in the ocean at different locations. Apart from this they should both be equal at the surface, which is also equal to the fresh water flux of $E-P-R$. This 'meeting' of the streamlines at the surface can be directly seen in Fig. 3 but to emphasise this we have graphed their surface values in Fig. 5 together with their zonally and meridionally integrated $E-P-R$. The match holds true, albeit with small dissimilarities north of 30°N, which might be due to the following three reasons. (1) The ORCA1 model grid is unstructured north of 30°N, which makes it impossible to have an exact latitude for the zonal integration in the ocean stream function. (2) The land masses are greater here than in the SH and the effect of rivers as explained above could play a role in that it would rain at a given latitude but the ocean river run-off would be at another. (3) The diffusive moisture fluxes have been omitted in the calculations. This discontinuity of the streamlines at the surface is, however, so small, that it does not affect our concluding results and it is therefore not necessary to speculate further into this for the present study.

3.2. Eddy-induced and mean-flow meridional atmospheric water circulation

To get a detailed dynamics of the meridional atmospheric water circulation, time averaged water-mass stream function has been divided into its mean-flow contribution and eddy-induced part (Fig. 6)

$$\psi^{atm}_{j,k} = \bar{\psi}_{j,k} + \psi'_{j,k}, \tag{14}$$

The mean-flow overturning stream function ($\bar{\psi}_{j,k}$) was computed from the time-mean flow field ($\bar{v}$) and time-mean pressure ($\overline{\Delta p}$) and specific humidity ($\bar{q}$) field distribution

$$\bar{\psi}_{j,k} = \sum_{k'=k}^{KL} \sum_{i=1}^{IX} \bar{q}_{i,j,k'} \bar{v}_{i,j,k'} \Delta x_{i,j} \overline{\Delta p}_{i,j,k'} / g. \tag{15}$$

The eddy-induced overturning water stream function ($\psi'_{j,k}$) was computed as the residual term using equation (14). It is clearly evident that mean-flow is the main contributor for transporting the atmospheric water equatorwards (0.38 Sv) due to the trade winds. Also, the mean-flow water circulation confined below 800 hPa. The transient eddies are the reason for water transport towards the mid- and high-latitudes from the tropics. In the Northern Hemisphere (NH), transient eddies are transporting 0.63 Sv of atmospheric water and in the SH this amount increases to 0.77 Sv. The mean-flow contribution can further be decomposed into zonal mean $\langle \psi_{j,k} \rangle$ part and stationary eddy (SE) and SE-zonal mean interactions (Fig. 7). The zonal overturning atmospheric water stream function $\langle \psi_{j,k} \rangle$ was computed from the zonal-mean flow field $\langle v \rangle$ and zonal-mean pressure $\langle \Delta p \rangle$ and specific humidity field $\langle q \rangle$ distribution

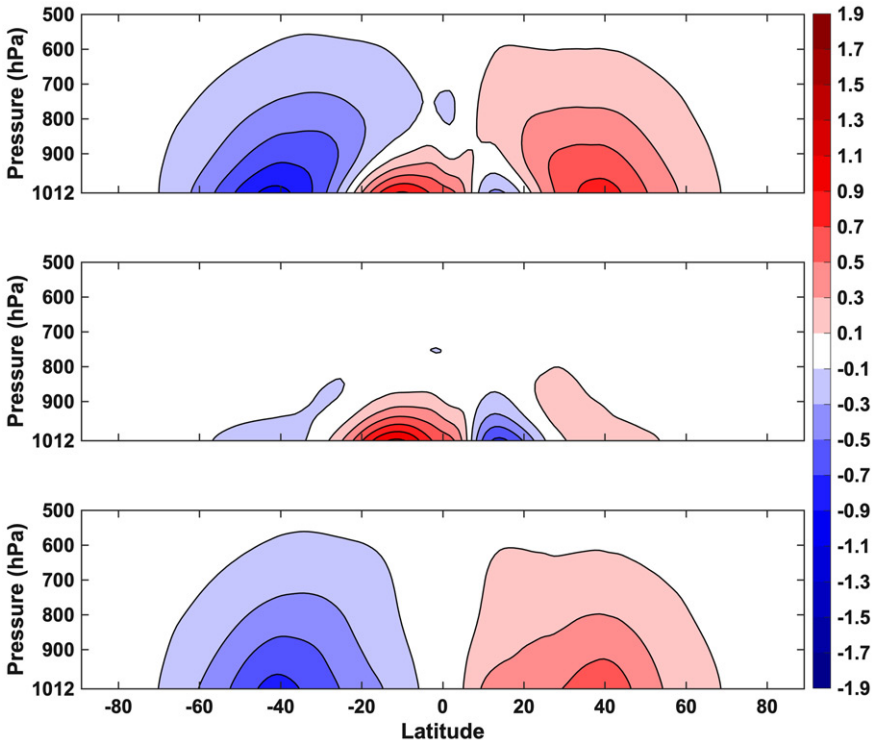

Fig. 6. Decomposition of the atmospheric water-mass stream function (top panel) into mean-flow (middle panel) and transient eddy contribution (bottom panel). All transports are in Sv (10^9 kg/s). Red cells correspond to clockwise circulation and blue to anti-clockwise circulation.

$$\langle \psi_{j,k} \rangle = IX * \frac{1}{N} \sum_{n=1}^{N} \sum_{k'=k}^{KL} \langle q^n_{j,k'} \rangle \langle v^n_{j,k'} \rangle \Delta x_j \langle \Delta p^n_{j,k'} \rangle / g. \qquad (16)$$

Zonal mean flow holds the largest share of the mean-flow equatorward transport (0.37 Sv). Stationary eddies and their interactions with the zonal mean flow are responsible for small amount of atmospheric water transport towards the equator (0.05 Sv). They also transport water towards the mid- and high-latitudes from the subtropics (0.17 Sv in NH and 0.09 Sv in SH) but the magnitude of this water transport is very tiny as compared to the transient eddies.

3.3. The hydrological cycle in a warmer climate

The ocean–atmosphere water-mass stream function for the RCP 8.5 scenario has also been calculated and compared with that of the present-day climate. This in order to estimate possible future changes of the complete hydrological cycle (Fig. 8).

Although the large scale patterns of the water-mass cells remain unchanged, the amplitude of the hydrological cycle intensified in the future climate scenario (cf. increased number of streamlines in Fig. 8 as compared with the present-day-climate simulation of Fig. 3). To quantify this amplification, the maximum and minimum values of the present-day-climate stream function at the surface were taken in each hemisphere and compared with those of the future climate. In the NH, there will be a 15% increase in the equatorward moisture transport and a 20% increase of the poleward moisture transport compared to the present-day climate. Similarly in the SH, equatorward moisture transport is an increase in the future climate scenario by 27% and poleward transport of moisture amplification by 20%. The moisture transport increment in the future climate scenario is compensated by an ocean return flow in the opposite direction. Note that, the cross-Equatorial flow of moisture increased by 0.2 Sv (34%) in the future-climate scenario (one additional streamline in Fig. 8 compared to Fig. 3 across the Equator). This extra 0.2 Sv of moisture transport across the Equator in the future climate scenario mainly feeds the North Pacific with more precipitation. The water then arrives at the deep water formation sites at the northern North Atlantic and joins the sinking branch of the North Interhemispheric Cell.

4. Conclusions

In the present study, the atmospheric water-mass stream function of Peixoto and Oort (1992) has been introduced

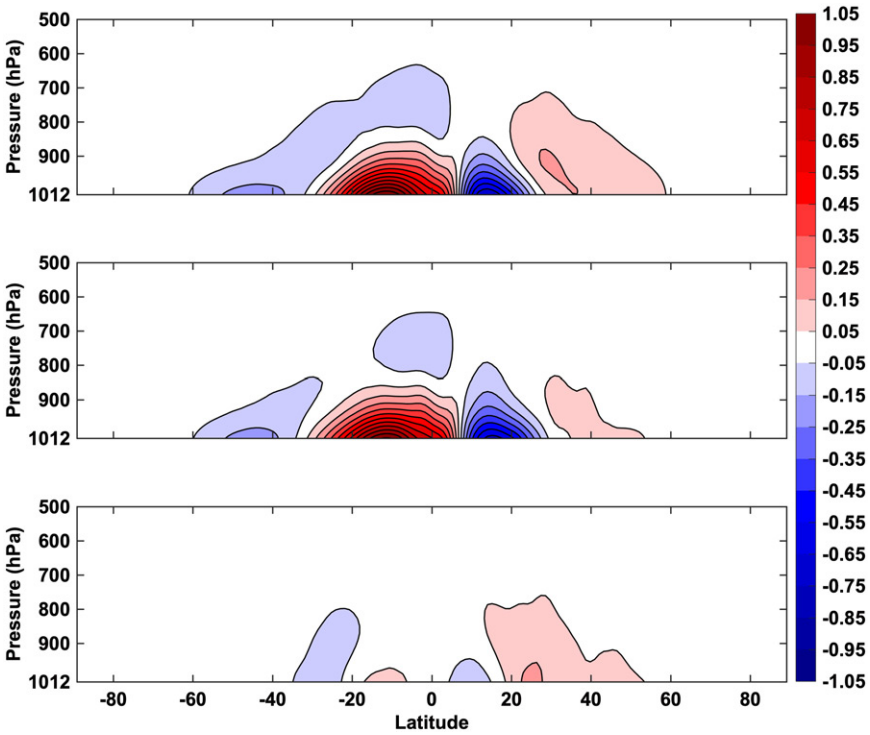

Fig. 7. Decomposition of the mean-flow atmospheric water-mass stream function (top panel) into zonal mean flow (middle panel) and stationary eddy-zonal mean interactions contribution (bottom panel). All transports are in Sv (10^9 kg/s). The mean-flow atmospheric water-mass stream function here is the same as in Fig. 6 middle panel, but with different contour interval.

to trace the hydrological cycle through the atmosphere, down into the ocean and back up into the atmosphere, resulting in a complete hydrological cycles, with corresponding water-mass cells. The streamlines of these ocean–atmosphere cells should be interpreted as a water-mass redistribution not as individual Lagrangian trajectories. This holds true for any type of ocean or atmosphere overturning stream function, since only streamlines in a steady non-divergent 2D flow are parallel to trajectories.

Ocean overturning stream lines are always open at the surface due to $E-P-R$, but the calculation of the atmospheric water-mass stream function using this novel method made it possible to close these open streamlines by following them up in the atmosphere and back down into the ocean.

It is important to emphasise that the present study is a mass budget analysis and when the atmospheric freshwater precipitates it will first affect the sea surface salinity and then merge with the ocean overturning circulation. Although this freshwater flux from the atmosphere is one order of magnitude less than that of the ocean it plays a crucial role in the thermohaline circulation by redistributing the salinity. The six ocean–atmosphere cells should be interpreted as a mass budget distribution not necessarily as actual water paths.

Six atmospheric water-mass cells were discovered, which are connected with the oceanic overturning cells through the sea surface. The atmospheric streamlines start at the Earth's surface where evaporation exceeds precipitation and terminate where precipitation exceeds evaporation. Similarly, these streamlines continue into the ocean from where precipitation exceeds evaporation and return to the surface where evaporation exceeds precipitation, hereby closing the water-mass cells. The six complete ocean–atmosphere water cells shown schematically in Fig. 4 are the following. The two *Tropic Cells* are confined near the surface in both the ocean and the atmosphere. A striking feature is that the water streamlines are in opposite direction to those of the Hadley Cells in the lower part of the ITCZ, which is simply the precipitation falling against the ascending air.

The two *Hemispheric Cells* transport moisture at lower altitudes in the atmosphere towards the ITCZ from the evaporative subtropics by the lower branch of the Hadley Cells. Then at higher altitude the moisture travels poleward into the Ferrel Cells, where the transient eddies carry the moisture until they precipitates at the higher latitudes. Once in the ocean they will first flow equatorward as Ekman transport until they downwell and merges with

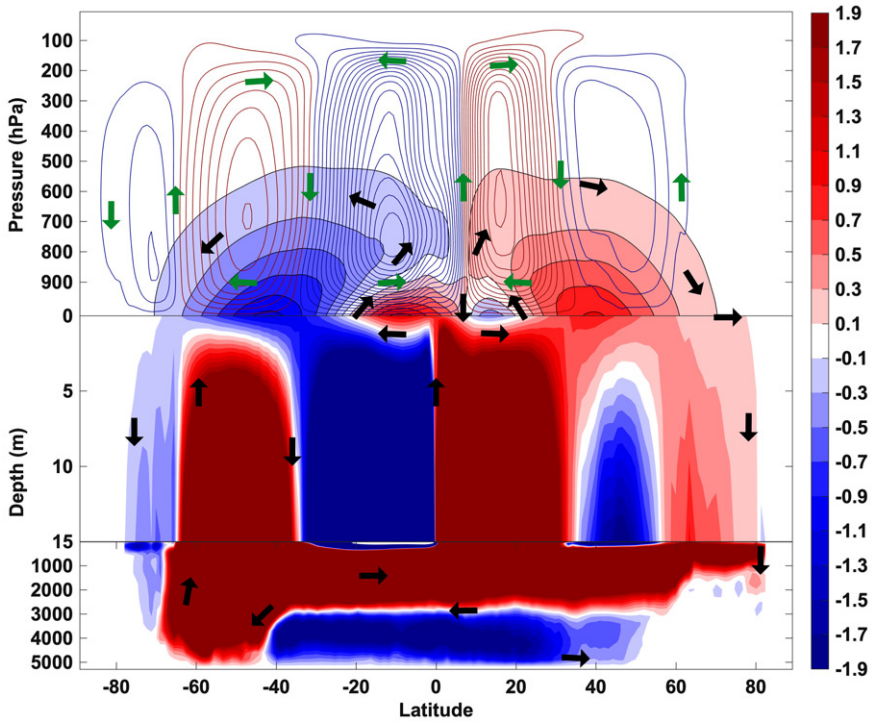

Fig. 8. The global water-mass overturning stream function for the coupled ocean–atmosphere system superimposed with the global air-mass overturning stream function for the future climate (RCP 8.5). Black arrows shows the water-mass transport direction and green arrows indicate the air-mass transport direction. All transports are in Sv (10^9 kg/s). Note that the colour scale is saturated. Contour interval for air-mass transport is 6 Sv.

the ocean Tropical Cells. These ocean tropical cells upwell at the Equator, where the water is once again in the Ekman layer but now driven away from the Equator until evaporating and thus closes the cells. The *North Interhemispheric Cell* is a complex water cycle, which is southward in the ocean and northward in the atmosphere. The *South Interhemispheric Cell* is in the ocean merged with the AABW Cell and hence crosses back and forth the Equator in the deep ocean. It also merges with the South Hemispheric Cell. Under the influence of the warmer climate, these coupled water-mass cells will increase their strength (increased number of streamlines).

To better understand the dynamics behind the atmospheric water transport, a Reynolds decomposition was applied on the atmospheric meridional water overturning stream function. It was found that mean-flow is mainly responsible for the equatorward water transport and associated with the lower branch of the Hadley cells. Transient eddies (synoptic weather systems) are the driving factor for atmospheric water transport towards the mid- and high-latitudes. Mid-latitude Ferrel and Polar cells are insignificant in transporting atmospheric water towards the higher latitudes as compared with the transient and stationary eddies.

A possible continuation of the present atmospheric water-mass transport study could be to extend it in the zonal direction with both water-mass stream functions and Lagrangian water-mass trajectories connecting the ocean basins though the atmosphere. This could get some insight into how the salinity differences of the ocean basins are directly related to the redistribution of freshwater through not only the ocean currents but also the winds.

Acknowledgements

The authors wish to thank Peter Lundberg for constructive comments. We are grateful for discussions on this work with Aitor Aldama Campino and Sara Berglund. The EC-Earth model integrations and the Eulerian stream function computations were performed on resources provided by the Swedish National Infrastructure for Computing (SNIC) at the National Supercomputer Centre at Linköping University (NSC).

Disclosure statement

No potential conflict of interest was reported by the authors.

References

Blanke, B., Arhan, M. and Speich, S. 2006. Salinity changes along the upper limb of the Atlantic thermohaline circulation. *Geophys. Res. Lett.* **33**, L06609. doi:10.1029/2005GL024938

Bryan, K. 1991. Ocean circulation models. *Strateg. Future Climate Res.* **29**, 265–286.

Döös, K. and Nilsson, J. 2011. Analysis of the meridional energy transport by atmospheric overturning circulations. *J. Atmos. Sci.* **68**, 1806–1820. doi:10.1175/2010JAS3493.1

Döös, K., Nilsson, J., Nycander, J., Brodeau, L. and Ballarotta, M. 2012. The world ocean thermohaline circulation. *J. Phys. Oceanogr.* **42**, 1445–1460. doi:10.1175/JPO-D-11-0163.1

Döös, K. and Webb, D. J. 1994. The deacon cell and the other meridional cells of the southern ocean. *J. Phys. Oceanogr.* **24**, 429–442. doi:10.1175/1520-0485(1994)024<0429:TDCATO>2.0.CO;2

Emile-Geay, J., Cane, M. A., Naik, N., Seager, R., Clement, A. C. and van Geen, A. 2003. Warren revisited: Atmospheric freshwater fluxes and? Why is no deep water formed in the north pacific? *J. Geophys. Res.* **108**(C6), 3178. doi:10.1029/2001JC001058

England, M. H. 1992. On the formation of Antarctic intermediate and bottom water in ocean general circulation models. *J. Phys. Oceanogr.* **22**, 918–926. doi:10.1175/1520-0485(1992)022<0918:OTFOAI>2.0.CO;2

Ferrari, R. and Ferreira, D. 2011. What processes drive the ocean heat transport? *Ocean Modell.* **38**, 171–186. doi:10.1016/j.ocemod.2011.02.013

Ferreira, D. and Marshall, J. 2015. Freshwater transport in the coupled ocean–atmosphere system: a passive ocean. *Ocean Dyn.* **65**, 1029–1036. doi:10.1007/s10236-015-0846-6

Gill, A. and Bryan, K. 1971. Effects of geometry on the circulation of a three-dimensional southern-hemisphere ocean model. *Deep Sea Res. Oceanograph. Abs.* **18**, 685–721. doi:10.1016/0011-7471(71)90086-6

Hazeleger, W., Severijns, C., Semmler, T., Ştefănescu, S., Yang, S. and co-authors. 2010. Ec-earth: A seamless earth-system prediction approach in action. *Bull. Am. Meteorol. Soc.* **91**, 1357–1364. doi:10.1175/2010BAMS2877.1

Hazeleger, W., Wang, X., Severijns, C., Ştefănescu, S., Bintanja, R. and co-authors. 2012. Ec-earth v2. 2: Description and validation of a new seamless earth system prediction model. *Clim. Dyn.* **39**, 2611–2629. doi:10.1007/s00382-011-1228-5

Held, I. M. and Soden, B. J. 2006. Robust responses of the hydrological cycle to global warming. *J. Climate* **19**, 5686–5699. doi:10.1175/JCLI3990.1

Huntington, T. G. 2006. Evidence for intensification of the global water cycle: Review and synthesis. *J. Hydrol.* **319**, 83–95. doi:10.1016/j.jhydrol.2005.07.003

Lorenz, D. J. and DeWeaver, E. T. 2007. The response of the extratropical hydrological cycle to global warming. *J. Climate* **20**, 3470–3484. doi:10.1175/JCLI4192.1

Madec, G. 2008. *Nemo reference manual, ocean dynamic component: Nemo-opa*. Note du Pôle de modélisation, Institut Pierre Simon Laplace, France, Technical Report, 27.

Manabe, S., Bryan, K. and Spelman, M. J. 1975. A global ocean–atmosphere climate model. Part I. The atmospheric circulation. *J. Phys. Oceanogr.* **5**, 3–29. doi:10.1175/1520-0485(1975)005<0003:AGOACM>2.0.CO;2

Manabe, S., Bryan, K. and Spelman, M. J. 1990. Transient response of a global ocean–atmosphere model to a doubling of atmospheric carbon dioxide. *J. Phys. Oceanogr.* **20**, 722–749. doi:10.1175/1520-0485(1990)020<0722:TROAGO>2.0.CO;2

Pauluis, O., Czaja, A. and Korty, R. 2008. The global atmospheric circulation on moist isentropes. *Science* **321**, 1075–1078. doi:10.1126/science.1159649

Pauluis, O., Czaja, A. and Korty, R. 2010. The global atmospheric circulation in moist isentropic coordinates. *J. Climate* **23**, 3077–3093. doi:10.1175/2009JCLI2789.1

Peixoto, J. P. and Oort, A. H. 1992. *Physics of Climate*. American Institute of Physics, New York, 520 pp.

Trenberth, K. E., Fasullo, J. T. and Mackaro, J. 2011. Atmospheric moisture transports from ocean to land and global energy flows in reanalyses. *J. Climate* **24**, 4907–4924. doi:10.1175/2011JCLI4171.1

Trenberth, K. E. and Guillemot, C. J. 1998. Evaluation of the atmospheric moisture and hydrological cycle in the NCEP/NCAR reanalyses. *Climate Dyn.* **14**, 213–231. doi:10.1007/s003820050219

Warren, B. A. 1983. Why is no deep water formed in the north pacific? *J. Mar. Res.* **41**, 327–347. doi:10.1357/002224083788520207

Wetherald, R. T. and Manabe, S. 1972. Response of the joint ocean–atmosphere model to the seasonal variation of the solar radiation. *Mon. Wea. Rev.* **100**, 42–59. doi:10.1175/1520-0493(1972)100<0042:ROTJOM>2.3.CO;2

Yang, H., Li, Q., Wang, K., Sun, Y. and Sun, D. 2015. Decomposing the meridional heat transport in the climate system. *Clim. Dyn.* **44**, 2751–2768. doi:10.1007/s00382-014-2380-5

Zhu, Y. and Newell, R. E. 1998. A proposed algorithm for moisture fluxes from atmospheric rivers. *Mon. Wea. Rev.* **126**, 725–735. doi:10.1175/1520-0493(1998)126<0725:APAFMF>2.0.CO;2

Zika, J. D., England, M. H. and Sijp, W. P. 2012. The ocean circulation in thermohaline coordinates. *J. Phys. Oceanogr.* **42**, 708–724. doi:10.1175/JPO-D-11-0139.1